Sustained Lobe Reconnection in Saturn's Magnetotail

M. F. Thomsen[(1)], C. M. Jackman[(2)], D. G. Mitchell[(3)], G. Hospodarsky[(4)], W. S. Kurth[(4)], and K. C. Hansen[(5)]

[(1)] Planetary Science Institute, Tucson, AZ

[(2)] University of Southampton, Southampton, UK

[(3)] Applied Physics Laboratory, Johns Hopkins University, Laurel, MD

[(4)] University of Iowa, Iowa City, IA

[(5)] University of Michigan, Ann Arbor, MI

Abstract

The degree to which solar wind driving may affect Saturn's magnetosphere is not yet fully understood. We present observations that suggest that under some conditions the solar wind does govern the character of the plasma sheet in Saturn's outer magnetosphere. On 16 September 2006, the Cassini spacecraft, at a radial distance of 37 Rs near local midnight, observed a sunward-flowing ion population for ~5 hours, which was accompanied by enhanced Saturn Kilometric Radiation emissions. We interpret this beam as the outflow from a long-lasting episode of Dungey-type reconnection, i.e., reconnection of previously-open flux containing magnetosheath material. The beam occurred in the middle of a several-day interval of SKR activity and enhanced lobe magnetic field strength, apparently caused by the arrival of a solar-wind compression

This is the author manuscript accepted for publication and has undergone full peer review but has not been through the copyediting, typesetting, pagination and proofreading process, which may lead to differences between this version and the Version of Record. Please cite this article as doi: 10.1002/2015JA021768

region with significantly higher than average dynamic pressure. The arrival of the high-pressure solar wind also marked a change in the composition of the plasma-sheet plasma, from water-group-dominated material clearly of inner-magnetosphere origin to material dominated by light-ion composition, consistent with captured magnetosheath plasma. This event suggests that under the influence of prolonged high solar wind dynamic pressure, the tail plasma sheet, which normally consists of inner-magnetospheric plasma, is eroded away by ongoing reconnection that then involves open lobe field lines. This process removes open magnetic flux from the lobes and creates a more Earth-like, Dungey-style outer plasma sheet dominantly of solar wind origin. This behavior is potentially a recurrent phenomenon driven by repeating high-pressure streams (corotating interaction regions) in the solar wind, which also drive geomagnetic storms at Earth.

I. Introduction

The dynamics of the Earth's magnetosphere are well known to be driven dominantly by conditions in the incident solar wind plasma and magnetic field. At Saturn, strong internal magnetic fields, rapid planetary rotation, and the dominance of plasma sources deep within the magnetosphere (the moon Enceladus) combine to create magnetospheric dynamics that are strongly driven by internal plasma production and centrifugal forces. The degree to which solar wind driving may also affect Saturn's magnetosphere has thus not been entirely clear. There is some evidence that Earth-like coupling may occur, but its strength and consequences are still something of a mystery.

One way the solar wind may affect Saturn's magnetospheric dynamics is via viscous processes that operate near the magnetopause. For example, Kelvin-Helmholtz (K-H) waves driven by the flow shear at the magnetopause can lead to nonlinear vortices that relax through intermittent, small-scale reconnection [e.g., Walker et al., 2011; Ma et al., 2015]. Good evidence for K-H instability at Saturn's magnetopause has in fact been identified [e.g., Delamere et al., 2013], and this mechanism may provide a means to transfer part of the internally produced magnetospheric plasma (sourced primarily by the moon Enceladus) to the solar wind. It might also enable the magnetosphere to recapture some fraction of magnetic flux that is opened during dayside reconnection. However, it is not yet clear how such a boundary process could affect dynamics deeper in the magnetosphere.

Aside from such viscous boundary processes, the primary observational evidence suggesting that there is a solar wind influence has been twofold: 1) evidence for magnetopause reconnection and 2) the effects of solar wind dynamic pressure. We now touch briefly on each of these.

Magnetopause reconnection. Magnetopause reconnection at the Earth allows the direct transfer of solar wind energy and plasma into the magnetosphere: Open magnetic flux loading into the magnetotail lobes drives tail reconnection that both returns re-closed magnetic flux and traps solar wind plasma within the plasma sheet, forming the dominant constituent of magnetospheric plasma beyond the plasmasphere. This is the so-called

"Dungey cycle" of plasma and field circulation, and the presence of plasma of solar wind origin is one of the key pieces of evidence supporting it.

In situ evidence of the occurrence of magnetic reconnection at Saturn's magnetosphere has been reported [e.g., Huddleston et al., 1997; McAndrews et al., 2008; Lai et al., 2012; Masters et al., 2012; Badman et al., 2013; Jasinski et al., 2014; Fuselier et al., 2014], in spite of the fact that the typically high plasma beta in Saturn's magnetosheath and strong flow shears at low latitudes probably tend to inhibit its occurrence, except where the magnetic shear is high [Masters et al., 2012; Desroche et al., 2013; Fuselier et al., 2014].

Remote observations of Saturn's auroral oval also indicate the existence of dayside reconnection [e.g., Badman et al., 2005; Belenkaya et al., 2008, 2011; Radioti et al., 2011]. The existence of the dark polar cap is taken to be evidence of open magnetic field lines, and the size of the polar cap has been used to estimate the amount of open magnetic flux, with its time variation describing the imbalance between magnetopause reconnection that opens flux and tail reconnection that re-closes it [Badman et al., 2014]. In situ observations from several Cassini instruments during the high-inclination orbits between 2006 and 2009 [Jinks et al., 2014] found that the open/closed field-line boundary (the polar cap boundary) identified by the different in-situ observational signatures generally agreed with each other to within an average of ~0.34˚ of colatitude but typically resided poleward of the upward field-aligned current region that would correspond to the precipitation boundary identified remotely as the polar cap boundary. Thus, the true

region of open magnetic flux in the polar region is probably somewhat smaller than estimated by, e.g., Badman et al. [2014].

However, despite these indications that magnetopause reconnection does occur, the inferred reconnection electric field at the magnetopause seldom appears to be large enough to directly drive much in the way of magnetospheric dynamics [Masters et al., 2014]. Depending on the assumed length of the magnetopause reconnection line, Masters et al. estimate that the reconnection voltage is only rarely as high as 100 kV. They note that even for an x-line spanning the entire dayside magnetopause, the reconnection voltage exceeds 180 kV only ~22% of the time. The value of 180 kV is what Badman and Cowley [2007] estimate is required for solar-wind-driven flux transport to become competitive with the flux transport in the outer magnetosphere that is driven by coupling to Saturn's rotating ionosphere.

Solar wind dynamic pressure. The properties of the solar wind all vary substantially at the distance of Saturn's orbit [e.g., Crary et al., 2005; Zieger and Hansen, 2008, and references therein; Jackman and Arridge, 2011b]. Important indications of Saturn's magnetospheric response to the solar wind are the strong relationships between solar wind dynamic pressure and both Saturn kilometric radio emissions (SKR) [e.g., Desch, 1982; Kurth et al., 2005; Jackman et al., 2010] and the UV power of the aurorae [e.g., Clarke et al., 2005; Crary et al., 2005]. Cowley et al. [2005] suggested that the SKR and auroral brightenings in response to increased solar wind dynamic pressure might be due to compression-induced tail reconnection, involving Dungey-cycle closure

of lobe magnetic flux analogous to Earth's widely-studied magnetospheric response to corotating solar wind interaction regions (CIRs). Bunce et al. [2005] reported an example of such solar wind compression-induced reconnection on the outbound pass of the Cassini Saturn Orbit Insertion Maneuver. The remote observations of the polar cap size mentioned above support this speculation in that they show that open flux at Saturn is typically closed in relatively small events (few GWb), with occasional larger flux closure events associated with solar wind compressions [Badman et al., 2014].

Dungey-cycle vs. Vasyliunas-cycle. As noted above, the opening of magnetic flux at the dayside magnetopause requires an eventual re-closing of that flux, presumably in the tail, but there are a number of reasons why this Dungey-cycle circulation may not be very prominent at Saturn. We mentioned above the factors acting to inhibit or slow down dayside reconnection. In the tail, the strong outward centrifugal stresses on internally mass-loaded flux tubes act counter to the Dungey-cycle convection that would deliver re-closed flux to the inner magnetosphere [e.g., Thomsen, 2013]. The more likely tendency, described for Jupiter by Vasyliunas [1983], is for the closed, centrifugally-stretched, mass-loaded flux tubes to reconnect internally, allowing the loss of magnetospheric mass through the formation and ejection of a plasmoid [e.g., Jackman et al., 2015, and references therein]. This so-called "Vasyliunas cycle" satisfies the magnetosphere's need to shed plasma mass that is continuously produced in the inner magnetosphere. However, because it involves re-connection of already-closed field lines, it can not affect the balance of open and closed magnetic flux in the magnetosphere. If flux is opened at

the magnetopause and not closed there in small-scale viscous process, it must be closed in some sort of Dungey-cycle process, and it is important to understand how and where this can happen at Saturn.

There is now a great deal of evidence for the occurrence of Vasyliunas-cycle reconnection in Saturn's magnetosphere, including direct observation of departing plasmoids in the magnetotail [e.g., Jackman et al., 2007, 2014; Hill et al., 2008]. Delamere et al. [2015] have even argued that smaller-scale Vasyliunas-type reconnection occurs commonly throughout the dayside and dusk sectors. The in situ evidence for the operation of the Dungey cycle has been considerably sparser. The planet-ward consequences of tail reconnection have certainly been seen, in the form of in situ and remote observations of energized plasma and the dipolarization of reconnected flux returning to the inner magnetosphere [e.g., Bunce et al., 2005; Mitchell et al., 2005; Russell et al., 2008; Hill et al., 2008; Masters et al., 2013; Jackman et al., 2013, 2015; Thomsen et al., 2013, 2015;]. In addition, the strong association of SKR enhancements and extensions to lower frequencies with other signatures of tail reconnection (e.g., plasmoids [Jackman et al., 2009] and energetic particle injections [Bunce et al., 2005; Mitchell et al., 2005]) is attributed to low-altitude emissions produced during the dipolarization. But both Vasyliunas-cycle and Dungey-cycle tail reconnection should produce dipolarization and energization, so the challenge is to identify observational discriminants between the two processes.

One potentially clear diagnostic of Dungey vs. Vasyliunas is the ion composition of the injected plasma [e.g., Badman and Cowley, 2007]: The presence of W+ in the injected plasma is a strong indication that the reconnection occurred on previously-closed field lines, loaded with magnetospheric plasma (Vasyliunas cycle). By contrast, plasma trapped in the magnetosphere by reconnection of lobe field lines (Dungey cycle) should be dominantly of solar-wind composition. W+ has indeed been observed in several reported dipolarization events [Mitchell et al., 2005; Thomsen et al., 2013, 2015; Jackman et al., 2015], but so far injected plasma that lacks this inner-magnetospheric signature has not been reported, except possibly for a brief interval adjacent to an event with a clear Vasyliunas-cycle signature [Thomsen et al., 2015].

The principal in situ evidence suggesting the occurrence of nightside Dungey-cycle reconnection that returns magnetic flux to the magnetosphere is the extended interval of northward magnetic field that is often observed to follow plasmoid passage [Jackman et al., 2011, 2015]. Referred to as the post-plasmoid plasma sheet (PPPS) in analogy to similar features in the Earth's magnetotail [Richardson et al., 1987], this northward field is interpreted as the tailward exhaust from lobe reconnection that follows the initial reconnection of closed plasmasheet field lines (which resulted in release of the plasmoid). Thus, the suggestion is that an interval of Vasyliunas-cycle reconnection "clears away" the stressed, mass-loaded portion of the plasma sheet that inhibits lobe reconnection, allowing open lobe field lines finally to close and return via the Dungey cycle [see also Jia et al., 2012; Thomsen, 2013]. Such post-plasmoid lobe reconnection

has also been seen in global MHD simulations [Jia et al., 2012]. Indeed, it may actually be responsible for the fast departure velocity of the departing plasmoid [e.g., Jia et al., 2012; Thomsen et al., 2013; Mitchell et al., 2015].

In this paper we present observations from one of Cassini's 2006 tail orbits, in which we have found compelling evidence for a sustained interval of Dungey-cycle reconnection in Saturn's magnetosphere. For ~5 hours on 15-16 September 2006, Cassini observed a fast planet-ward flow similar to that reported by Jackman et al. [2015], who interpreted it as the signature of quasi-steady reconnection occurring tailward of the spacecraft. In contrast to the Jackman event, however, the flow reported here was almost totally composed of light ions (H+, m/q=2), with only a hint of W+ at quite high energies, as is commonly seen in the magnetosheath. Moreover, this reconnection signature occurred during a few-day interval of apparent compression of the magnetosphere by high solar-wind dynamic pressure (based on increased lobe field strength and propagated solar wind properties), with concomitant enhanced SKR activity. The character and composition of the tail plasma sheet changed dramatically from before the pressure enhancement to after its onset. This event suggests that under the influence of prolonged high solar wind dynamic pressure, the tail plasma sheet, normally consisting of inner-magnetospheric plasma, is eroded away by ongoing Vasyliunas-cycle reconnection that continues on to involve lobe field lines, creating a more Earth-like, Dungey-style outer plasma sheet dominantly of solar wind origin. This behavior is

potentially a recurrent phenomenon driven by high-pressure streams in the solar wind, which are also known to drive recurrent geomagnetic storms at Earth.

The observations presented here were obtained with four different instruments onboard the Cassini spacecraft: The Cassini Plasma Spectrometer (CAPS) [Young et al., 2004]; the Magnetic Field Investigation (MAG) [Dougherty et al., 2004]; the Magnetospheric Imaging Instrument (MIMI) [Krimigis et al., 2004]; and the Radio and Plasma Wave Science instrument (RPWS) [Gurnett et al., 2004]. The CAPS and MIMI/CHEMS (Charge Energy Mass Spectrometer) energy ranges (1 eV to ~50 keV and 3 to 326 keV, respectively) give overlapping coverage that enables us to track fast ion flows from typical plasma sheet speeds to the accelerated flows encountered in reconnection events [e.g., Jackman et al., 2015].

II. Sunward Ion Flow: 15-16 Sep 2006 (days 258-259)

Overview. Late on 15 Sept 2006 (day 258) Cassini was travelling outbound through Saturn's magnetotail plasma sheet near midnight local time, at a radial distance of 36.5 Rs and a latitude of 14.5°. Figure 1 summarizes the observations for the 12-hour interval beginning at 21 UT on 15 Sept. From top to bottom, the figure presents CAPS electron and ion observations, magnetic field measurements in KRTP coordinates, MIMI/CHEMS H+ and O+ energy spectra, and the frequency spectrum of the electric field component observed by RPWS.

In Figure 1a, from about 2120 on day 258 until 2300, the very low counts in the electron and ion spectrograms, combined with the relatively strong and smooth magnetic field that is largely in the radial direction (Figure 1c-f), show that Cassini was in the northern tail lobe. This identification is supported by the RPWS observation of low-frequency (<100 Hz) emissions (Figure 1i). At ~2300 a faint but energetic population was seen in both the ions and electrons (Figures 1a and 1b). The ions seen in the CAPS Ion Mass Spectrometer (IMS) in Figure 1b at that time were also seen in CHEMS, which identified them as dominantly H+ (Figure 1g), with essentially no O+ (Figure 1h). About 40 minutes later a denser and somewhat less energetic plasma population appeared (Figures 1a-b), which persisted for close to 4 h. At the end of this interval (~0320 UT), the ions and electrons both suddenly rose in energy by an order of magnitude, before the spacecraft briefly re-entered the lobe (0420-0500 UT).

The interval shown in Figure 1 occurred during a period of significant magnetospheric activity, as indicated by the intense SKR emissions seen in Figure 1i near 10^5 Hz. The SKR enhancement began earlier, near 1400 UT on day 258 (at which time Cassini was located at a radial distance ~36 Rs and latitude ~15˚, very near local midnight), and Figure 1i shows a number of re-intensifications, including near 0000 UT and 0400 UT. These two re-intensifications occurred less than an hour after the onset of the ion population noted above and of the onset of the sharp rise in ion energy, respectively.

Saturnward flow. The narrow thermal spread of the ions between 2300 and 0420 in Figure 1 suggests that they comprised a directional beam, rather than a hot, isotropic population. Figure 2 confirms this impression by showing the all-sky angular distribution of the ion population seen in CAPS at 0121-0126 UT on day 259. The ion counts are strongly confined near the center of the all-sky distribution, which in this figure is centered on the look direction that is opposite to Saturn. It it also very near the instantaneous magnetic field direction (solid dot), which at this time was pointed radially away from Saturn (see Panel 1d). As denoted by the red-colored bar above Figure 1a, this strong Saturnward flow characterized the ions seen in CAPS throughout the entire interval from 2300 to 0420 UT, including the current sheet crossing (Br reversal) at ~0230 in Figure 1. An upper limit to the flow speed can be obtained by assuming that the ion thermal energy is small compared to the flow energy, and for the interval in Figure 1 from ~0000 to 0330 UT, the upper-limit flow speed inferred from the energy of the ion spectral peak varied between ~200 and 500 km/s, rising to 1000-2000 km/s in the higher-energy intervals before 0000 and after 0300 UT. This conversion from energy to flow speed is based on the assumption that the dominant ions in the peak are H+, which is justified in the next paragraph. The CAPS numerical moments analysis [Thomsen et al., 2010] finds an H+ density for this interval declining from ~0.05 cm-3 at 0000 UT to ~0.02 cm-3 at ~0320 UT. With the relative densities for W+ and m/q=2 found from the TOF analysis we are about to discuss, we find a mass density for this population to be ~0.033-0.085 amu/cm3. The magnetic field strength near the lobe during this interval

was ~3.3 nT and in the current sheet was ~0.8 nT. These values lead to an Alfven speed ~60-400 km/s, quite comparable to the estimated flow speed.

Composition. We mentioned above that the faint ion distribution at the exit from the lobe at ~2300 UT was composed dominantly of H+, with very little discernible O+. Thereafter, until the beam energy began to rise at ~0320 UT, neither CAPS nor CHEMS saw significant amounts of water-group ions. Figure 1h shows only a smattering of O+ counts in CHEMS, distributed throughout the spectrum. This is in contrast to the H+ counts shown in Figure 1g, which show a broad enhancement below ~10 keV. The primary beam in CAPS (Figure 1b) is at ~1 keV, and there is no evidence for a second energy peak at 16 times that value, which is where O+ that shared the same flow speed as the H+ would appear.

Figure 3 summarizes the CAPS composition determination for the entire interval from 2340 to 0300 UT. Figure 3a shows the counts recorded during this interval in the matrix of energy and time-of-flight (TOF) channels from the IMS. The light blue curves indicate the range of TOF at each energy level that is occupied by each of the three principal species (H+, m/q=2, and W+, where "W" represents the water products O, OH, H_2O, and H_3O), as described by Thomsen et al. [2014]. As inferred from the non-mass-resolved spectra shown in Figure 1b, W+ counts are extremely sparse and broad in energy extent, suggesting a very tenuous and very hot distribution.

Figure 3b shows the densities of the three species inferred from the data shown in Figure 3a. The three curves show the contribution to the average density for each species

in each CAPS energy channel as a function of channel energy. The calculation of these values is described elsewhere [Thomsen et al., 2014]. That calculation assumes isotropy of the distribution, whereas the observed distribution is fairly well collimated (Figure 2), so the estimated absolute density is likely to be wrong, but the relative densities of the different species should be reasonably accurate if they share a similar angular distribution. The ratios of estimated densities are 0.034 and 0.044 for (m/q=2):H and W:H, respectively. These values are very much lower than is typically seen in plasma sheet material of inner magnetospheric origin (~0.1-1 and ~0.1-10, for m/q=2 and W, respectively [e.g., Thomsen et al., 2010]). In particular, the (m/q=2):H ratio is more characteristic of the solar wind plasma (few percent) than of magnetospheric plasma. The value of W:H is not only much lower than normally seen in the plasma sheet, but because no background subtraction has been done in this density estimate, the true ratio is likely to be even lower than this.

It is well known that the water-group plasma in Saturn's magnetotail is strongly confined to the equatorial plane by centrifugal forces [e.g., Szego et al., 2011, 2012], so it is possible that the lack of W+ in the sunward-flowing ions seen between 2340 and 0300 UT is due to a latitude effect. We examine this possibility in Figure 4a, which shows that even during the current sheet crossing at 0230 UT (Br reversal, Figure 1d), the CAPS ion spectrum shows no hint of enhanced fluxes at energies above the main light-ion population. At this time, as in Figure 2, the ions were strongly flowing Saturn-ward, and water-group ions flowing at the same speed as the H+ would have had energies ~10 keV.

Not only are such ions not seen in CAPS, but CHEMS also sees very few O+ counts near ~10 keV at this time (Figure 1). Thus, we can be confident that the W+ content of the plasma sheet during this fast-flow event was extremely low, at least up until ~0320 UT.

Referring again to Figure 1, at ~0320 UT the beam energy rose rather sharply, and entered the CHEMS energy range, where a strong enhancement of H+ flux was observed. At the same time significant fluxes of O+ were observed by CHEMS between 10 and 20 keV. CAPS also detected these water-group ions as a second peak in the energy spectrum, as seen more clearly in Figure 4b. Figure 1a shows that the electron temperature increased during this interval, and ion moments calculations (not shown) indicate that both the ion speed and the temperature increased.

Magnetic field. Throughout most of the beam interval in Figure 1 the magnetic field was fairly smooth and largely in the radial direction (Figures 1c-f). The current sheet crossing, as determined from a sharp change in the sign of Br, occurred at ~0230 UT on day 259. The change in Br is by far the most significant field signature at this time. The total field strength after the crossing was higher than before, due primarily to increases in Bθ and Bϕ. Bϕ also changed sign at the crossing, so that the usual anti-phase Br-Bϕ relationship was retained. At the onset of the rise in beam energy at ~0320 UT (red dashed line in Figures 1c-f), Br decreased from a smooth, lobe-like -4 nT, to a noisier, outer-plasma-sheet-like -2 nT. Bθ also began to fluctuate considerably at this time, turning very briefly and very slightly northward but quickly returning to positive values, reaching ~1.5 nT at ~03:30 and ~1.75 nT just after 05:00. The fluctuations in the

field appear similar to fluctuations typically seen in the high-beta plasma sheet. The overall direction of Bθ at this time was southward, and Br indicated that Cassini was below the current sheet. The reduced magnitude of Br and the stronger Bθ indicate a reduction in the stretching of the field and a more dipolar orientation.

Vasyliunas-type reconnection. In Figure 1 there is a clear change in the character of the observations starting at 0320 UT. The field dipolarization, combined with the fast Saturn-ward flow speed (Vr up to ~-160 km/s at 0330, with an azimuthal speed ~100 km/s, well below the full corotational value of 355 km/s), the increased plasma temperature (from T_H~300 eV to >2 keV), and the subsequent onset of enhanced SKR emissions strongly suggest active reconnection activity tailward of Cassini, as previously reported by other investigators [e.g., Bunce et al., 2005; Thomsen et al., 2013, 2015]. The clear presence of water-group ions indicates that the reconnection was occurring on previously closed field lines (Vasyliunas-type).

Comparison with Jackman et al. [2015]. The main beam event presented in Figure 1 (2300-0320 UT) is in many respects quite similar to the ion flow event described recently by Jackman et al. [2015] and attributed also to magnetic reconnection occurring in the tail beyond the distance of the spacecraft. Like that event, the strong Saturn-ward flow and the associated onset of SKR activity indicate that we are seeing the outflow from a long-lasting tail reconnection episode (~5 h, compared to ~1.5 h in the Jackman et al. event).

The ion energy in the present event is lower than that in the Jackman event, as is the electron temperature, but the principal difference between this event and that one is the ion composition: In the event presented here, we find almost no water-group ions, whereas in their event, Jackman et al. found clear evidence of significant amounts of O+, co-flowing with the sunward population of H+. The O+ was not seen in CAPS in their event because the fast flow and high mass shifted the population into the CHEMS energy range. In the event discussed here, no such co-flowing O+ population could be found until the flow changed character at ~0320 UT, at which point both CAPS and CHEMS observed significant fluxes of O+, and both the beam speed and temperature increased. At that point, which was also nearly concurrent with another SKR enhancement, the event in Figure 1 much more nearly resembled the one reported earlier.

Because of the clear presence of O+ in the Saturnward flow, Jackman et al. [2015] interpreted their event as indicative of a long-lasting Vasyliunas-type process, involving tail reconnection of already-closed magnetic flux and the shedding of a large plasmoid. In our case, as we will discuss in more detail below, the composition evidence suggests that the ion beam shown in Figure 1 is most likely the outflow from a long-lasting episode of Dungey-type reconnection, i.e., reconnection of previously-open flux containing magnetosheath material (until the change in composition and character of the flow at ~0320 UT indicate a return to a Vasyliunas-type process). We now consider the broader context in which this beam was observed.

III. Larger Context: 29 Aug – 21 Sep 2006 (day 241-264)

Figure 5 presents 24 days of data for the interval surrounding the ion beam event described above. Figure 5a shows the magnitude of the magnetic field measured by Cassini as it passed from near apoapsis on day 241 through periapsis on day 252 to several days past the following apoapsis on day 260. The interval presented in Figure 1 lies between the vertical dashed lines. The red dashed curve in Figure 5a shows the average lobe magnetic field strength at Cassini's location, as derived from magnetometer measurements during the tail orbits between days 18 and 291 of 2006 [Jackman and Arridge, 2011a]. The solid bars at the top of Figure 5a indicate time periods when CAPS electron measurements indicated that Cassini was either in the lobe or in the very low-density outer plasma sheet, where the plasma pressure is so low that the magnetic field has the same strength as in the adjacent lobe. In general, at any given radial distance the field in the lobe is higher than inside the plasma sheet, where thermal pressure can contribute to overall pressure balance. Therefore, the measured lobe field strength for the interval in Figure 5a is roughly the upper envelope of the black curve.

Figure 5b shows the electric field power spectrum observed by RPWS during the same interval. In this figure black, blue, and green represent progressively larger wave power. Figure 5c gives the solar wind dynamic pressure at Saturn estimated with the University of Michigan mSWIM 1.5-D MHD model, with solar wind conditions as observed at 1 AU as a boundary condition [Zieger and Hansen, 2008]. For this model, the most reliable predictions are found to occur within 75 days of apparent conjunction

between the Earth and Saturn. Apparent conjunction occurred on day 56 of 2006 and day 70 of 2007, so the interval investigated here is not ideally timed in this respect. However, 2006 was characterized by a very high solar wind recurrence index [Zieger and Hansen, 2008]; under such conditions the predictions are likely to be quite reasonable even half a year away from the time of apparent opposition, with the RMS error in shock arrival times found to be ~30-50 h [Zieger and Hansen, 2008]. The horizontal lines in Figure 5a indicate the various percentile levels of the dynamic pressure predicted for Saturn by mSWIM during the entire year of 2006 (see also Jackman and Arridge [2011b]).

Comparison of the observed magnetic field magnitude in Figure 5a with the average lobe field strength from Jackman and Arridge [2011a] shows that prior to day 245 the peak measured field strengths were comparable to the average lobe field. Starting at the beginning of day 245, however, the peak observed field, including within the actual lobe, fell well below that average lobe field, by as much as a factor of 2. This transition corresponded closely to a sharp drop in the mSWIM-predicted solar wind dynamic pressure, from near its median value for the year to near its fifth percentile level. Thus, both the observed field and the predicted dynamic pressure strongly suggest that Saturn's magnetosphere was immersed in a solar wind rarefaction region at that time and was in a significantly de-compressed state.

During Cassini's periapsis passage (~days 251-254), the predicted dynamic pressure rose dramatically, to nearly the 95th percentile level. Thereafter, it remained largely above average, except for a brief interval on day 259. Indeed, the lobe magnetic

field values observed by Cassini after periapsis are clearly well above the long-term average, indicating that during the second half of the time period shown in Figure 5, Saturn's magnetosphere was in a highly compressed state.

At about the time that the mSWIM results predict a major increase in the solar wind dynamic pressure, while Cassini was going through periapsis, there was a major increase in the intensity and lower-frequency extent of the SKR emissions (Figure 5c). During the periapsis pass itself, the interpretation of the SKR occurrence can be confused by shadow effects near the equatorial plane at close range, especially in the afternoon sector [Lamy et al., 2008; Galopeau et al., 1989]. Once the spacecraft returned to the night-side plasma sheet, from which the SKR viewing was probably good, there were a number of repeated episodes of enhanced intensity and extension to lower frequencies. These episodes appear to occur at or just after particularly strong lobe field intervals. The occurrence of SKR enhancements in association with solar wind pressure increases is well established, as mentioned above. The association of SKR emissions with magnetotail reconnection signatures is also well established. Hence it seems clear that in response to the increased solar wind dynamic pressure during Cassini's periapsis pass, Saturn's magnetotail entered an interval of frequent reconnection activity.

Figure 6 shows the same content as Figure 5, but for the more limited time range of day 255 to day 259. The association of enhanced SKR emissions with intervals of enhanced pressure (i.e., stronger than average magnetic field intensity) is clear. Indeed, on this scale it appears that the SKR onsets occur shortly after the peaks in the lobe

magnetic field intensity (see vertical red lines identifying maxima in the field strength), i.e., during times when the lobe pressure was declining after an enhancement. Jackman et al. [2010] noted a similar association between decreases in the lobe field strength and the onset of SKR enhancements. They further showed that the flaring angle of the magnetopause decreased in concert with the overall field strength. They attributed the increased flaring they inferred during lobe field increases as due to the loading of new magnetic flux into the lobes through enhanced magnetopause reconnection. By inference, the episodic decreases in |**B**| and the flaring angle would result from a closure of lobe flux through Dungey-cycle reconnection. It is interesting to note that the average time between inferred reconnection episodes is ~11 hr, suggesting that planetary rotation continues to play a role in the timing of Saturn magnetotail reconnection, as inferred by previous authors.

In addition to the substantial change in the character of the magnetic field and in the magnetospheric activity level (SKR), another striking magnetospheric change from the low dynamic pressure conditions before periapsis to the high pressure after periapsis was seen in the nature of the plasma sheet. Figure 7 illustrates two crossings of the current sheet (i.e., Br reversals) at approximately the same spatial location, one from pre-periapsis and the other from post-periapsis. Panels a and b show the CAPS/SNG ion energy-time spectrograms for the two time intervals, and panels c and d show the corresponding computations of the densities from the TOF data according to the method

of Thomsen et al. [2014]. The green and red arrows on the time axes of panels a and b indicate the approximate times at which the current sheet was crossed.

A visual comparison of Figures 7a and 7b makes it immediately clear that before periapsis, the central plasma sheet at this distance was rich in water-group ions relative to the H+ content. The derived densities and density ratios shown in panels c and d quantify this difference. The pre-periapsis central plasma sheet was rich in both water-group ions and ions with m/q=2 (presumably H2+), relative to the H+ content. Such plasma is characteristic of Saturnian magnetospheric plasma [e.g., Thomsen et al., 2010]. By contrast, the post-periapsis central plasma sheet has very little water-group plasma, and the ratio of m/q=2 to H+ is much more typical of solar wind plasma than Saturn's magnetosphere.

By selecting both examples in Figure 7 from near current sheet crossings, we avoid the possibility that the composition differences we see are attributable to the strong latitude dependence of heavy ions mentioned above [e.g., Szego et al., 2011, 2012]. To demonstrate that the differences between the two plasma-sheet crossings of Figure 7 were in fact characteristic of the plasma sheet prior to and after periapsis, Figure 8 shows a concatenation of two-hour CAPS spectrogram segments from all the current sheet crossings by Cassini between day 240 and day 263 for which there were detectable ions in CAPS IMS. The energy scale (not shown) is the same as Figures 7a and 7b. The green and red arrows indicate the 2-h segments illustrated in Figures 7a and 7b, respectively.

Prior to periapsis (i.e., above the "periapsis" line in Figure 8), the ion spectra are qualitatively similar to Figure 7a in that there are generally two clear peaks in E/q, corresponding to H+ at lower energies and W+ at higher energies. After periapsis (below the line in Figure 8), the character of the ion distributions is quite different. Before mid-day on day 261, there is only one crossing where there is a clear W+ peak. In the remaining crossings there is little evidence for a second peak, and moreover the H+ peak is typically much broader in energy (i.e., the population is hotter) than prior to periapsis. After mid-day on day 261, the plasma-sheet ions return to the character they displayed prior to periapsis, with a clear and persistent W+ peak. Note that mid-day on day 261 is also the time beyond which the lobe magnetic field strength no longer indicated a state of magnetospheric compression (Figure 5).

IV. Discussion

The similarity of the Saturn-ward ion beam event of Figure 1 to events previously described in the literature [e.g., Bunce et al., 2005; Thomsen et al., 2013, 2015; Jackman et al., 2015] indicates that magnetic reconnection was occurring in Saturn's magnetotail beyond the location of Cassini for ~5 hours. Jackman et al. [2015] presented an event that demonstrated quasi-steady tail reconnection over a time span of at least 1.5 hours, and Arridge et al. [in press, 2015] have shown evidence for ongoing but time variable tail reconnection over ~18 hours. Thus, it seems clear that while reconnection in the tail does occur episodically, releasing plasmoids as described extensively in the literature [e.g.,

Jackman et al., 2007, 2009, 2011, 2014; Hill et al., 2008], it also at times occurs in a more persistent, quasi-steady manner as well.

The principal difference between the ion beam event presented here and that reported by Jackman et al. [2015] is the relative absence of water-group ions in the Saturn-ward flowing population. Since W+ must originate in the inner magnetosphere of Saturn, its presence in the outflow from a reconnection region is taken to be diagnostic for Vasyliunas-type reconnection. The absence of significant W+ in the event presented here (at least prior to the energization episode at ~0320 UT) therefore suggests the possibility that this is mantle plasma emerging from a Dungey-type reconnection of lobe field lines. This possibility is strengthened by the fact that the ratio of (m/q=2) ions to H+ ions is appreciably lower than the typical H2+:H+ ratio within the magnetosphere and much more comparable to the He++:H+ ratio within the solar wind.

We used the term "relative absence of water-group ions" above because both CAPS and MIMI did see some W+ during this interval (c.f., Figure 3). However, not only did it comprise less than a few percent of the plasma density, but it had quite a different spectral character than is typically seen in the outflow from Vasyliunas-type reconnection [e.g., Thomsen et al., 2013; 2015; Jackman et al., 2015; see also the energized plasma observed after 0320 UT in Figure 1]. It was quite hot and tenuous, with weak counts spread across a broad range of energies. We suggest that this W+ may actually be present in the mantle plasma that is captured by Dungey-cycle tail reconnection. Sergis et al. [2013] have shown that substantial fluxes of W+ are present in

Saturn's magnetosheath, even dominating the total population above 50 keV at times. As a magnetosheath ion component, this W+ would be expected to populate open lobe field lines along with the magnetosheath plasma of solar wind origin (H+ and He++). Thus, when lobe magnetic flux reconnects, hot W+ should be recaptured on newly-closed field lines, and probably further heated in the process. Such recaptured W+ should be more tenuous and hotter than W+ delivered directly to the tail plasma sheet on closed field lines moving outward from the inner magnetosphere.

While the above discussion emphasizes the low W+ content of most of the beam event observed in Figure 1, the change in composition and spectral properties at ~0320 UT noted above indicates that intervals of Vasyliunas-type reconnection can continue in the midst of ongoing Dungey-type reconnection. Presumably this is because the general corotational flow, which typically remains strong even at these mid-tail distances [e.g., McAndrews et al., 2009; Thomsen et al., 2010, 2013], is continually delivering filled or partially filled flux tubes into the night-side tail. When a longitudinal sector arrives that has not recently undergone disconnection and plasmoid formation, it might now be stressed to the point of reconnection and downtail plasmoid release.

The beam event of Figure 1 occurred during a several-day interval of enhanced solar wind dynamic pressure, as indicated by the above-average lobe field strength and confirmed by predictions from the mSWIM solar wind propagation model (Figure 5). The mSWIM results indicate that the solar wind dynamic pressure enhancement was part of a large-scale solar-wind stream structure and that it followed a several-day rarefaction

interval, which was similarly reflected in the lower-than-average lobe field strength observed by Cassini in the days preceding the interval of Figure 1.

During the extended interval of enhanced solar wind dynamic pressure, SKR activity was enhanced, in agreement with previous observations, showing that high solar wind pressure triggers an extended period of tail reconnection. During the pre-periapsis rarefaction interval, SKR activity was present but at a relatively low level, and no major enhancements or expansions to lower frequency were observed. For the interval displayed in Figure 6, the onset of the SKR enhancement and expansion to lower frequency seems clearly associated with maxima in the lobe field strength, suggesting that the onset of tail reconnection reduces the lobe field pressure and flaring angle by removing magnetic flux from the lobe and returning it planet-ward.

The onset of the extended interval of tail reconnection associated with the arrival of the high-pressure solar wind also marked a significant change in the character of the tail plasma sheet probed by Cassini: During the pre-periapsis rarefaction interval, the central plasma sheet (near the current sheet crossings) clearly contained substantial quantities of thermal W+ ions, the normal content of the plasma sheet dominated by material originating in the inner magnetosphere. During the post-periapsis compression interval, little thermal W+ was seen, with only a few exceptions. The central plasma sheet was dominated by light ions, with only a very hot and tenuous contribution from W+. As just mentioned, we suggest that this W+ may have been present in the magnetosheath plasma captured in the reconnection of lobe field lines. The very low

ratio of (m/q=2) ions to H+ in the post-periapsis central plasma sheet further supports the conclusion that the plasma sheet in this interval is dominantly formed by Dungey-type reconnection of lobe field lines, with the (m/q=2) contribution primarily attributable to solar wind He++.

The above observations confirm previous observational and theoretical evidence that the arrival of a solar-wind compression region triggers an extended interval of tail reconnection [e.g., Bunce et al., 2005; Cowley et al., 2005; Jackman et al., 2010; Jia et al., 2012; Badman et al., 2014]. As noted previously [e.g., Thomsen et al., 2013], closure of lobe flux is inhibited by the strong centrifugal stress on mass-loaded flux tubes carrying inner magnetospheric plasma in the plasma sheet. Therefore, to close lobe flux the magnetosphere must first shed mass through Vasyliunas-type reconnection and plasmoid formation. Thereafter, with the centrifugal stress relieved, the reconnection can proceed into the lobes, initiating Dungey-style closure of lobe flux and capture of mantle plasma. The result is the reduction of open flux [e.g., Badman et al., 2014] and the creation of a light-ion dominated outer plasma sheet, as observed here.

We can estimate the magnetic flux transfer rate occurring in the magnetotail during this episode by combining the observed Saturnward flow velocities determined above for the interval from 0000 to 0300 on day 259 with the observed theta component of the magnetic field. For a flow speed between 200 and 500 km/s and a theta component between ~0.1 and 0.6 nT (before and after the 0230 current sheet crossing), we find a flux transfer rate of ~1.2-18 kV/Rs (0.02-0.30 mV/m). While we don't really know how wide

the tail reconnection line might be, an x-line of width 25 Rs would correspond to a total reconnection voltage ~30-450 kV, comparable to the 180 kV needed to compete with ionospheric-driven flux transport [Badman and Cowley, 2007]. Persisting for these three hours, such a reconnection line would return ~0.3-4.9 GWb of magnetic flux to the closed field line region. This is a significant fraction of the 10-15 GWb of open polar cap flux that is observed to be closed on timescales of ~20 h under solar wind compression conditions [Badman et al., 2014].

As seen in Figure 8, the light-ion domination of the outer plasma sheet persisted for at least ~3 days after the first post-periapsis encounter with the tail current sheet. It may well have begun earlier, but Cassini was not in a good position to observe the plasma sheet content then. In any case, this event demonstrates that Dungey-type reconnection can proceed for extended periods of time under the influence of strong solar-wind compression events. Thus, while much of Saturn's magnetospheric dynamics is dominated by internal plasma production and the rapid planetary rotation, the solar wind can at times assert control over the tail dynamics and formation of the outer plasma sheet, more like the Earth's magnetosphere.

The large solar wind dynamic pressure variations inferred during the interval reported here are not isolated temporal features; rather they appear to be part of a recurrent global solar wind structure. Zieger and Hansen [2008] have noted that during 2006, near the end of the declining phase of the solar sunspot cycle, when recurrent high-speed stream structure is typically seen, the solar wind observed at Earth's orbit had the

highest recurrence index since 1975. This index, defined by Zieger and Hansen, is a measure of the repeatability of the solar wind speed from one 27-d Bartels rotation to the next. This high recurrence in the 1-AU boundary condition of the mSWIM model carries through to the predicted solar wind properties at Saturn, as illustrated in Figure 9, which shows a stack of 50-day plots of the mSWIM-predicted solar wind dynamic pressure for the year. Each panel represents roughly two full solar rotations (note that the synodic solar rotation period at Saturn is closer to the sidereal rate than at the Earth's orbit). Periapsis on day 252, which immediately preceded the compression interval we have been examining, is marked with an arrow in the next-to-bottom panel in the figure. The recurrent stream structure of the solar wind is clear from Figure 9, with one major high-speed stream during each solar rotation for most of the year (possibly involving a merger of 2 or more interaction regions [e.g., Hanlon et al., 2004]), evolving into ~3 smaller streams by the end of the year. The linear scale of Figure 9 obscures the fact that the trough-to-peak variation in dynamic pressure ranged from 1 to 2 orders of magnitude (see also the percentile levels presented in Figure 5c).

Figure 9 thus suggests that the sequence of dynamical events we describe in this paper may represent a recurrent stream-driven state of the magnetosphere of Saturn, analogous to the well-studied CIR-driven geomagnetic storms at Earth. Current work in progress (Mitchell, personal communication) will demonstrate important evidence of that recurrent behavior.

V. Conclusions

The sunward ion beam observed by Cassini (Figure 1) in conjunction with enhanced SKR emissions confirms previous evidence that magnetotail reconnection at Saturn can be ongoing for at least several hours. The absence of a thermal W+ component and the solar-wind-like ratio of (m/q=2) to H+ suggest that the beam is the outflow from Dungey-type reconnection of open lobe field lines, rather than previously closed plasma sheet field lines (Vasyliunas-type). The presence of a hot (>30 keV), very tenuous W+ component is attributed to capture of W+ commonly found in magnetosheath plasma, rather than to material transported directly from the inner magnetosphere to the tail plasma sheet on closed field lines.

The beam occurs in the middle of a several-day interval of enhanced SKR activity and enhanced lobe magnetic field strength, apparently caused by the arrival of a solar-wind compression region with significantly higher than average dynamic pressure. Output from the mSWIM 1.5-D MHD simulation of solar wind properties confirms the likelihood of strong compression at this time.

The arrival of the high-pressure solar wind marks a change in the character of the plasma sheet plasma, from clearly of inner-magnetosphere origin to dominantly light-ion composition, consistent with captured magnetosheath plasma. This event suggests that under the influence of prolonged high solar wind dynamic pressure, the tail plasma sheet, which normally consists of inner-magnetospheric plasma, is eroded away by ongoing reconnection that continues on to involve lobe field lines. This process removes open

magnetic flux from the lobes and creates a more Earth-like, Dungey-style outer plasma sheet dominantly of solar wind origin. Such behavior was predicted by Cowley et al. [2005] and discussed more quantitatively by Badman and Cowley [2007] based on estimates of the magnetopause reconnection rate by Jackman et al. [2004]. Finally, as seen in Figure 9, the solar-wind dynamic pressure during this event was rather typical of the values found in the compression regions of recurrent corotating interaction regions, so, as noted explicitly by Cowley and colleagues, this magnetospheric response is potentially a recurrent phenomenon driven by repeating high-pressure streams in the solar wind, which also drive geomagnetic storms at Earth.

Acknowledgements

This work benefited greatly from discussions held during two meetings of the International Space Science Institute (ISSI) team on "Modes of Radial Transport in Magnetospheres." Work at PSI was supported by the NASA Cassini program through JPL contract 1243218 with Southwest Research Institute. The Cassini project is managed by the Jet Propulsion Laboratory for NASA. MFT is grateful to Los Alamos National Laboratory for the support provided her as a guest scientist. For this research DGM was supported by the NASA Office of Space Science under Task Order 003 of contract NAS5-97271 between NASA Goddard Space Flight Center and the Johns Hopkins University. The research at the University of Iowa was supported by NASA through Contract 1415150 with the Jet Propulsion Laboratory and NASA grant NNX12AG86G.

CMJ was supported by a Science and Technology Facilities Council Ernest Rutherford Fellowship. The CAPS and MIMI distributions, the magnetic field values, and the RPWS power spectra shown in this analysis are available from the Planetary Data System (http://pds.nasa.gov/). The mSWIM predictions of solar wind properties are publicly available on the University of Michigan web site (http://mswim.engin.umich.edu/). The authors thank both referees for very useful suggestions.

References

Arridge, C. S., et al. (2015), Cassini in situ observations of long duration magnetic reconnection in Saturn's magnetotail, *Nature Physics,* in press.

Badman, S. V., and S. W. H. Cowley (2007), Significance of Dungey-cycle flows in Jupiter's and Saturn's magnetospheres, and their identification on closed equatorial field lines, *Ann. Geophys., 25,* 941, doi:10.5194/angeo-25-941-2007.

Badman, S. V., E. J. Bunce, J. T. Clarke, S. W. H. Cowley, J.-C. Gérard, D. Grodent, and S. E. Milan (2005), Open flux estimates in Saturn's magnetosphere during the January 2004 Cassini-HST campaign, and implications for reconnection rates, *J. Geophys. Res., 110,* A11216, doi:10.1029/2005JA011240.

Badman, S. V., A. Masters, H. Hasegawa, M. Fujimoto, A. Radioti, D. Grodent, N. Sergis, M. K. Dougherty, and A. J. Coates (2013), Bursty magnetic reconnection at Saturn's magnetopause, *Geophys. Res. Lett., 40,* 1027–1031, doi:10.1002/grl.50199.

Badman, S. V., et al. (2014), Open flux in Saturn's magnetosphere, *Icarus, 231*, 137, doi:10.1016/j.icarus.2013.12.004.

Belenkaya, E. S., S. W. H. Cowley, S. V. Badman, M. S. Blokhina, and V.V. Kalegaev (2008), Dependence of the open-closed field line boundary in Saturn's ionosphere on both the IMF and solar wind dynamic pressure: comparison with the UV auroral oval observed by the HST, *Ann. Geophys., 26*, 159.

Belenkaya, E. S., S. W. H. Cowley, J. D. Nichols, M. S. Blokhina, and V. V. Kalegaev (2011), Magnetospheric mapping of the dayside UV auroral oval at Saturn using simultaneous HST images, Cassini IMF data, and a global magnetic field model, *Ann. Geophys., 29*, 1233.

Bunce, E. J., S. W. H. Cowley, D. M. Wright, A. J. Coates, M. K. Dougherty, N. Krupp, W. S. Kurth, and A. M. Rymer (2005), In situ observations of a solar wind compression-induced hot plasma injection in Saturn's tail, *Geophys. Res. Lett., 32*, L20S04, doi:10.1029/2005GL022888.

Clarke, J. T., et al. (2005), Morphological differences between Saturn's ultraviolet aurorae and those of Earth and Jupiter, *Nature*, *433*, 717–719, doi:10.1038/nature03331.

Cowley, S. W. H., S. V. Badman, E. J. Bunce, J. T. Clarke, J.-C. Gérard, D. Grodent, C. M. Jackman, S. E. Milan, and T. K. Yeoman (2005), Reconnection in a rotation-dominated magnetosphere and its relation to Saturn's auroral dynamics, *J. Geophys. Res.*, *110*, A02201, doi:10.1029/2004JA010796.

Crary, F. J., et al. (2005), Solar wind dynamic pressure and electric field as the main factors controlling Saturn's aurorae, *Nature, 433,* 720, doi:10.1038/nature/03333.

Delamere, P. A., R. J. Wilson, S. Eriksson, and F. Bagenal (2013), Magnetic signatures of Kelvin-Helmholtz vortices on Saturn's magnetopause: Global survey, *J. Geophys. Res., 118,* 393, doi: 10.1029/2012JA018197.

Delamere, P. A., A. Otto, X. Ma, F. Bagenal, and R. J. Wilson (2015), Magnetic flux circulation in the rotationally driven giant magnetospheres, *J. Geophys. Res., 120,* 4229, doi:10.1002/2015JA021036.

Desch, M. D. (1982), Evidence for solar-wind control of Saturn radio emission, *J. Geophys. Res., 87,* 4549.

Desroche, M., F. Bagenal, P. A. Delamere, and N. Erkaev (2013), Conditions at the magnetopause of Saturn and implications for the solar wind interaction, *J. Geophys. Res., 118,* 3087–3095, doi:10.1002/jgra.50294.

Dougherty, M. K., et al. (2004), The Cassini magnetic field investigation, *Space Sci. Rev., 114,* 331-383.

Fuselier, S. A., R. Frahm, W. S. Lewis, A. Masters, J. Mukherjee, S. M. Petrinec, and I. J. Sillanpaa (2014), The location of magnetic reconnection at Saturn's magnetopause: A comparison with Earth, *J. Geophys. Res., 119,* 2563–2578, doi:10.1002/2013JA019684.

Galopeau, P., P. Zarka, and D. Le Quéau (1989), Theoretical model of Saturn's kilometric radiation spectrum, *J. Geophys. Res., 94*(A7), 8739–8755, doi:10.1029/JA094iA07p08739.

Gurnett, D. A., et al. (2004), The Cassini radio and plasma wave investigation, *Space Sci. Rev., 114*, 395-463.

Hanlon, P. G., M. K. Dougherty, R. J. Forsyth, M. J. Owens, K. C. Hansen, G. Toth, F. J. Crary, and D. T. Young (2004), On the evolution of the solar wind between 1 and 5 AU at the time of the Cassini Jupiter flyby: Multispacecraft observations of interplanetary coronal mass ejections including the formation of a merged interaction region, *J. Geophys. Res., 109,* A09S03, doi:10.1029/2003JA010112.

Hill, T. W., et al. (2008), Plasmoids in Saturn's magnetotail, *J. Geophys. Res., 113*, A01214, doi:10.1029/2007JA012626.

Huddleston, D. E., C. T. Russell, G. Le, and A. Szabo (1997), Magnetopause structure and the role of reconnection at the outer planets, *J. Geophys. Res., 102*(A11), 24289–24302, doi:10.1029/97JA02416.

Jackman, C. M., and C. S. Arridge (2011a), Statistical properties of the magnetic field in the Kronian magnetotail lobes and current sheet, *J. Geophys. Res., 116,* A05224, doi:10.1029/2010JA015973.

Jackman, C.M., C.S. Arridge (2011b), Solar cycle effects on the dynamics of Jupiter's and Saturn's magnetospheres, *Solar Phys.*, *274*, 481-502, doi 10.1007/s11207-011-9748-z.

Jackman, C. M., et al. (2004), Interplanetary magnetic field at ~9AU during the declining phase of the solar cycle and its implications for Saturn's magnetospheric dynamics, *J. Geophys. Res., 109,* A11203, doi:10.1029/2004JA010614.

Jackman, C. M., C. T. Russell, D. J. Southwood, C. S. Arridge, N. Achilleos, and M. K. Dougherty (2007), Strong rapid dipolarizations in Saturn's magnetotail: In situ evidence of reconnection, *Geophys. Res. Lett., 34,* L11203, doi:10.1029/2007GL029764.

Jackman, C. M., L. Lamy, M. P. Freeman, P. Zarka, B. Cecconi, W. S. Kurth, S. W. H. Cowley, and M. K. Dougherty (2009), On the character and distribution of lower-frequency radio emissions at Saturn and their relationship to substorm-like events, *J. Geophys. Res., 114,* A08211, doi:10.1029/2008JA013997.

Jackman, C. M., et al. (2010), In situ observations of the effect of a solar wind compression on Saturn's magnetotail, *J. Geophys. Res., 115,* A10240, doi:10.1029/2010JA015312.

Jackman, C. M., J. A. Slavin, and S. W. H. Cowley (2011), Cassini observations of plasmoid structure and dynamics: Implications for the role of magnetic reconnection in magnetospheric circulation at Saturn, *J. Geophys. Res., 116,* A10212, doi:10.1029/2011JA016682.

Jackman, C.M., N. Achilleos, S.W.H. Cowley, E.J. Bunce, A. Radioti, D. Grodent, S.V. Badman, M.K. Dougherty, W. Pryor, Auroral counterpart of magnetic field

dipolarizations in Saturn's tail (2013), *Planet. Space Sci., 82-83*, 34-42, doi: 10.1016/j.pss.2013.03.010

Jackman, C. M., et al. (2014), Saturn's dynamic magnetotail: A comprehensive magnetic field and plasma survey of plasmoids and traveling compression regions and their role in global magnetospheric dynamics, *J. Geophys. Res., 119*, 5465–5494, doi:10.1002/ 2013JA019388.

Jackman, C. M., M. F. Thomsen, D. G. Mitchell, N. Sergis, C. S. Arridge, M. Felici, S. V. Badman, C. Paranicas, X. Jia, G. B. Hospodarksy, M. Andriopoulou, K. K. Khurana, A. W. Smith, and M. K. Dougherty (2015), Field dipolarization in Saturn's magnetotail with planetward ion flows and energetic particle flow bursts: Evidence of quasi-steady reconnection. *J. Geophys. Res., 120,* 3603–3617, doi:10.1002/2015JA020995.

Jasinski, J. M., et al. (2014), Cusp observation at Saturn's high-latitude magnetosphere by the Cassini spacecraft, *Geophys. Res. Lett., 41*, 1382–1388, doi:10.1002/2014GL059319.

Jia, X., et al. (2012), Magnetospheric configuration and dynamics of Saturn's magnetosphere: A global MHD simulation, *J. Geophys. Res., 117*, A05225, doi:10.1029/2012JA017575.

Jinks, S. L., et al. (2014), Cassini multi-instrument assessment of Saturn's polar cap boundary, *J. Geophys. Res., 119*, 8161, doi:10.1002/2014JA020367.

Krimigis, S. M., et al. (2004), Magnetosphere imaging instrument (MIMI) on the Cassini mission to Saturn/Titan, *Space Sci. Rev., 114*, 233-329.

Kurth, W. S., et al. (2005), An Earth-like correspondence between Saturn's auroral features and radio emission, *Nature, 433*, 722, doi:10.1038/nature03334.

Lai, H. R., H. Y. Wei, C. T. Russell, C. S. Arridge, and M. K. Dougherty (2012), Reconnection at the magnetopause of Saturn: Perspective from FTE occurrence and magnetosphere size, *J. Geophys. Res., 117*, A05222, doi:10.1029/2011JA017263.

Lamy, L., P. Zarka, B. Cecconi, R. Prangé, W. S. Kurth, and D. A. Gurnett (2008), Saturn kilometric radiation: Average and statistical properties, *J. Geophys. Res., 113*, A07201, doi:10.1029/2007JA012900.

Ma, X., B. Stauffer, P. A. Delamere, and A. Otto (2015), Asymmetric Kelvin-Helmholtz propagation at Saturn's dayside magnetopause, *J. Geophys. Res., 120*, 1867, doi:10.1002/2014JA020746.

Masters, A., J. P. Eastwood, M. Swisdak, M. F. Thomsen, C. T. Russell, N. Sergis, F. J. Crary, M. K. Dougherty, A. J. Coates, and S. M. Krimigis (2012), The importance of plasma β conditions for magnetic reconnection at Saturn's magnetopause, *Geophys. Res. Lett., 39*, L08103, doi:10.1029/2012GL051372.

Masters, A., M. F. Thomsen, S. V. Badman, C. S. Arridge, D. T. Young, A. J. Coates, and M. K. Dougherty (2011), Supercorotating return flow from reconnection in Saturn's magnetotail, *Geophys. Res. Lett., 38*, L03103, doi:10.1029/2010GL046149.

Masters, A., M. Fujimoto, H. Hasegawa, C. T. Russell, A. J. Coates, and M. K. Dougherty (2014), Can magnetopause reconnection drive Saturn's magnetosphere?, *Geophys. Res. Lett.*, *41*, 1862–1868, doi:10.1002/2014GL059288.

McAndrews, H. J., C. J. Owen, M. F. Thomsen, B. Lavraud, A. J. Coates, M. K. Dougherty, and D. T. Young (2008), Evidence for reconnection at Saturn's magnetopause, *J. Geophys. Res., 113*, A04210, doi:10.1029/2007JA012581.

McAndrews, H. J., M. F. Thomsen, C. S. Arridge, C. M. Jackman, R. J. Wilson, M. G. Henderson, R. L. Tokar, K.K. Khurana, E. C. Sittler, A. J. Coates, and M. K. Dougherty (2009), Plasma in Saturn's nightside magnetosphere and implications for global circulation, *Plan. Sp. Sci., 57*, 1714.

Mitchell, D. G., et al. (2005), Energetic ion acceleration in Saturn's magnetotail: Substorms at Saturn?, *Geophys. Res. Lett., 32*, L20S01, doi:10.1029/2005GL022647.

Mitchell, D. G., et al. (2015), Injection, Interchange, and Reconnection: Energetic Particle Observations in Saturn's Magnetosphere, in *Magnetotails in the Solar System*, ed. A. Keiling, C. M. Jackman, and P. A. Delamere, AGU Geophysical Monograph 207, John Wiley & Sons, 327-344.

Radioti, A., D. Grodent, J.-C. Gérard, S. E. Milan, B. Bonfond, J. Gustin, and W. Pryor (2011), Bifurcations of the main auroral ring at Saturn: ionospheric signatures of consecutive reconnection events at the magnetopause, *J. Geophys. Res., 116,* A11209, doi:10.1029/2011JA016661.

Richardson, I. G., S. W. H. Cowley, E. W. Hones Jr., and S. J. Bame (1987), Plasmoid-associated energetic ion bursts in the deep geomagnetic tail: Properties of plasmoids and the post-plasmoid plasma sheet, *J. Geophys. Res., 92*, 9997–10,013, doi:10.1029/JA092iA09p09997.

Russell, C. T., et al. (2008), Titan's influence on Saturnian substorm occurrence, *Geophys. Res. Lett., 35*, L15101.

Sergis, N., C. M. Jackman, A. Masters, S. M. Krimigis, M. F. Thomsen, D. C. Hamilton, D. G. Mitchell, M. K. Dougherty, and A. J. Coates (2013), Particle and magnetic field properties of the Saturnian magnetosheath: Presence and upstream escape of hot magnetospheric plasma, *J. Geophys. Res., 118,* 1620–1634, doi:10.1002/jgra.50164.

Szego, K., Z. Nemeth, G. Erdos, L. Foldy, M. Thomsen, and D. Delapp (2011), The plasma environment of Titan: The magnetodisk of Saturn near the encounters as derived from ion densities measured by the Cassini/CAPS plasma spectrometer, *J. Geophys. Res., 116,* A10219, doi:10.1029/2011JA016629.

Szego, K., Z. Nemeth, G. Erdos, L. Foldy, Z. Bebesi, M. Thomsen, and D. Delapp (2012), Location of the magnetodisk in the nightside outer magnetosphere of Saturn near equinox based on ion densities, *J. Geophys. Res., 117*, A09225, doi:10.1029/2012JA017817.

Thomsen, M. F. (2013), Saturn's magnetospheric dynamics, *Geophys. Res. Lett., 40*, 5337-5344, doi:10.1002/2013GL057967.

Thomsen, M. F., et al. (2010), Survey of ion plasma parameters in Saturn's magnetosphere, *J. Geophys. Res.*, *115*, *A10220*, *doi:*10.1029/2010JA015267.

Thomsen, M. F., et al. (2013), Cassini/CAPS observations of duskside tail dynamics at Saturn, *J. Geophys. Res.*, *118*, 5767–5781, doi:10.1002/jgra.50552.

Thomsen, M. F., et al. (2014), Ion composition in interchange injection events in Saturn's magnetosphere, *J. Geophys. Res.*, *119*, doi:10.1002/2014JA020489.

Thomsen, M. F., D. G. Mitchell, X. Jia, C. M. Jackman, G. Hospodarsky, and A. J. Coates (2015), Plasmapause formation at Saturn. *J. Geophys. Res.*, *120*, 2571–2583, doi:10.1002/2015JA021008.

Vasyliunas, V. M. (1983), Plasma distribution and flow, in *Physics of the Jovian Magnetosphere*, edited by A. J. Dessler, pp. 395-453, Cambridge Univ. Press, New York.

Walker, R. J., K. Fukazawa, T. Ogino, and D. Morozoff (2011), A simulation study of Kelvin-Helmholz waves at Saturn's magnetopause, *J. Geophys. Res.*, *116*, A03203, doi:10.1029/2010JA015905.

Young, D. T., et al. (2004), Cassini Plasma Spectrometer investigation, *Space Sci. Rev.*, *114*, 1–112.

Zieger, B., and K. C. Hansen (2008), Statistical validation of a solar wind propagation model from 1 to 10 AU, *J. Geophys. Res.*, *113*, A08107, doi:10.1029/2008JA013046.

Figure Captions

1. Sunward-flowing ion beam event observed by Cassini on 15-16 Sep 2006 (Days 258-259) near local midnight at ~37 Rs downtail: a) Electron count rate (proportional to energy flux) from CAPS/ELS; b) ion count rate (proportional to energy flux) from the singles (SNG) measurement of CAPS/IMS; c-f) total strength and KRTP components of the magnetic field observed by MAG, where B_R is positive above the current sheet, B_θ is positive southward, and B_ϕ is positive in the corotation direction; g) H+ and h) O+ count rate spectrograms from MIMI/CHEMS; and i) electric field power spectrum from RPWS. The bright emissions above ~10^4 Hz in panel i are identified as SKR. The colored bars above panel a show the lobe intervals and the interval in which a Saturnward ion flow was observed. The vertical red dashed line in panels c-f marks the transition to higher beam energies and a return to significant water-group composition.

2. All-sky angular distribution of ions observed by CAPS/IMS between 0121 and 0126 UT on day 259, taken at the energy of peak ion counts (1024 eV). The center of the angular distributions corresponds to the look direction away from Saturn, and the open triangle half-way to the outer circle on the right of center corresponds to the look direction into corotation. The counts are sharply peaked in the look direction away from Saturn, corresponding to strong Saturn-ward flow. The solid black dots show the direction of the magnetic field, and for this interval the flow is nearly field-aligned.

3. a) Ion counts observed by CAPS/IMS, sorted according to their energy and time of flight (TOF) in the instrument. Pairs of curves labeled H+, (m/q=2), and W+ indicate the range of TOF at each energy level that is populated by these species. The prominent peak below TOF~30 is an instrumental artifact, and the population near TOF~70 results from incident ions that strike the LEF MCP (see Thomsen et al. [2010] for a more complete discussion). The plot includes all the TOF data obtained during the ion beam event of Figure 1, from 2340 UT on day 258 to 0300 UT on day 259. b) Contribution to the total density of each species from each of the IMS energy channels averaged over the interval covered in panel a. Total densities are just the sum of the plotted contributions.

4. a) Energy-time spectrogram of non-mass-resolved ions (SNG) observed by CAPS/IMS for one hour centered on the current sheet crossing at ~0230 UT on day 259. There is a clear peak at ~600 eV corresponding to flowing H+, but no similar peak at ~10 keV, where one might expect co-flowing W+ to appear. b) Similar SNG spectrogram for the hour encompassing the strong energization (both inferred flow speed and temperature increased) after ~0320 UT on day 259. Plasma during this energization event had a clear contribution from co-moving W+, ~10-20 times the H+ peak energy.

5. a) Magnetic field magnitude and b) electric field power spectrum observed by Cassini over a 24-day interval containing the ion beam event of Figure 1 (marked by vertical dashed lines). The red dashed curve in (a) is the average lobe magnetic field magnitude determined by Jackman and Arridge [2011a], and the black bars at the top of that panel show times when Cassini was actually in or very near the lobe, based on CAPS/ELS

electron observations. c) Solar wind dynamic pressure predicted at Saturn for the same interval based on calculations of the mSWIM MHD model [Zieger and Hansen, 2008]. Horizontal lines indicate the various percentile values of the dynamic pressure calculated with this model for the entire year of 2006.

6. Same as Figure 5, for day 255 to day 259. SKR enhancements occur shortly after peaks in the magnetic field intensity, which are indicated by the vertical red dashed lines.

7. a) Ion energy-time spectrogram for a pre-periapsis crossing of the current sheet, showing the clear presence of two separate ion species (W+ at higher energies and light ions at lower energies). b) Similar spectrogram for a post-periapsis crossing of the current sheet. Only a light-ion peak is visible. c) Contribution to the total density of each species from each of the IMS energy channels, based on TOF measurements averaged over the interval covered in panel a. Total densities are the sum of the plotted contributions. Water-group ions are the dominant population, consistent with typical magnetospheric plasma observations. Ions with m/q=2 also have typical abundance for the outer magnetosphere. d) Same as (c) but for the interval in panel b. Water-group ions are extremely tenuous, and ions with m/q=2 have abundance much more similar to the solar wind than to typical magnetospheric plasma.

8. Concatenated 2-hour ion energy-time spectrograms for all the current-sheet crossings between the end of day 240 and the middle of day 263, and for which detectable ions were present in CAPS. The green and red arrows indicate the intervals highlighted in Figure 7. Prior to periapsis (above the black horizontal bar), the ion distribution was

characterized by two clear peaks in energy. After periapsis (below the bar), most of the distributions up until the middle of day 261 showed dominantly light ions, with little evidence for W+. After midday on day 261, the distribution returned to its pre-periapsis character.

9. Stack of 50-day plots of the solar wind dynamic pressure at Saturn predicted by mSWIM for the year 2006. For most of the year there was one prominent high-pressure stream during each solar rotation (~25 d). Near the end of the year, this recurrent stream structure evolved into 3 somewhat weaker streams. The arrow in the second panel from the bottom marks the Cassini periapsis immediately preceding the ion flow interval on days 258-259.

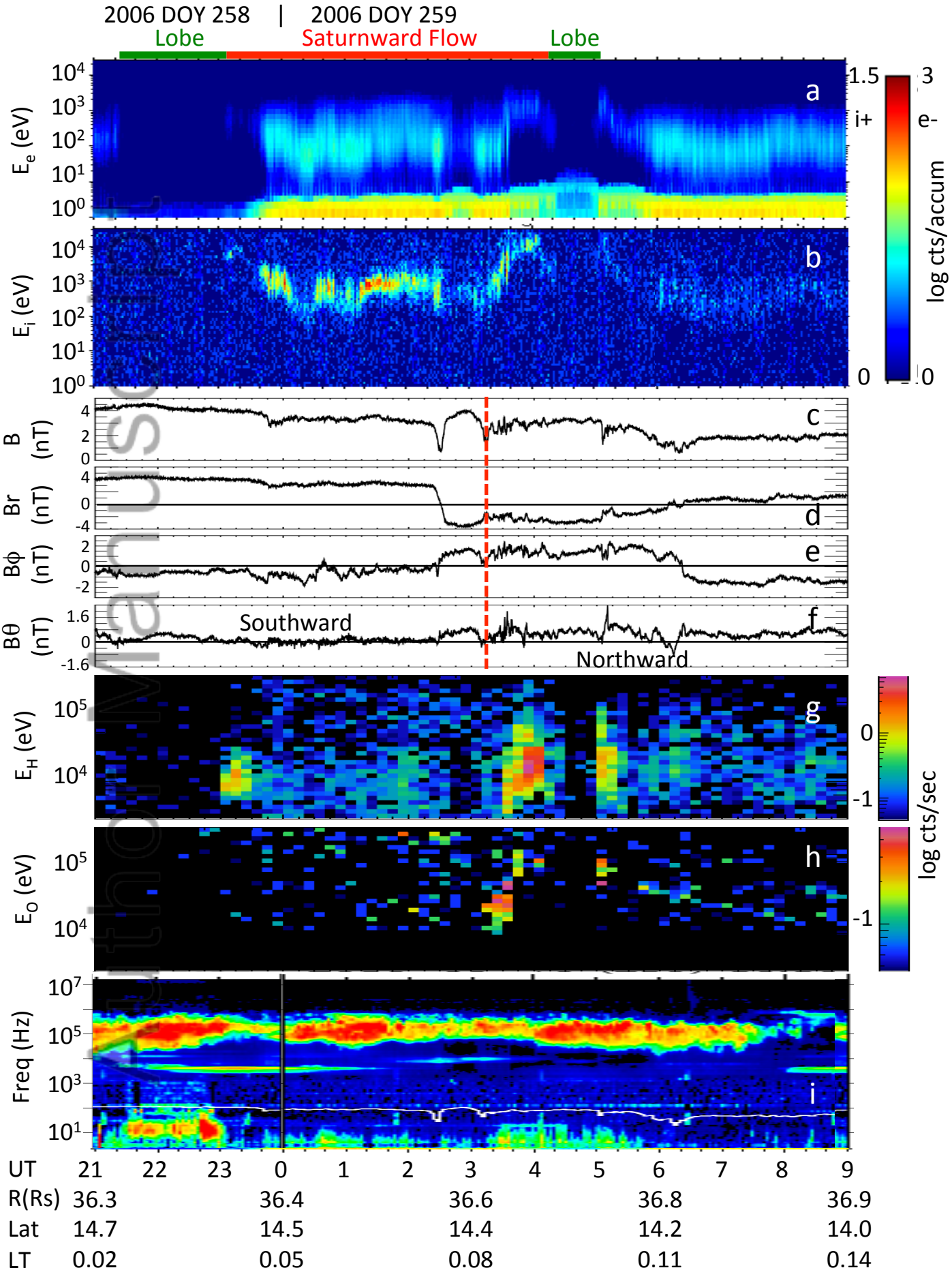

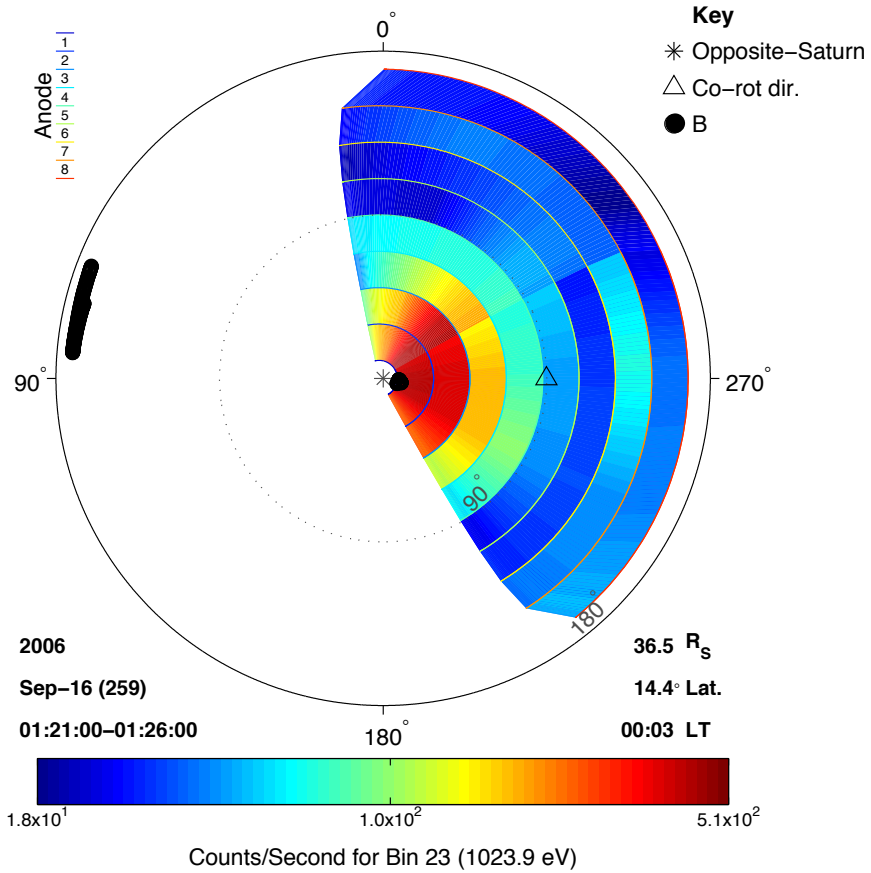

Figure 2

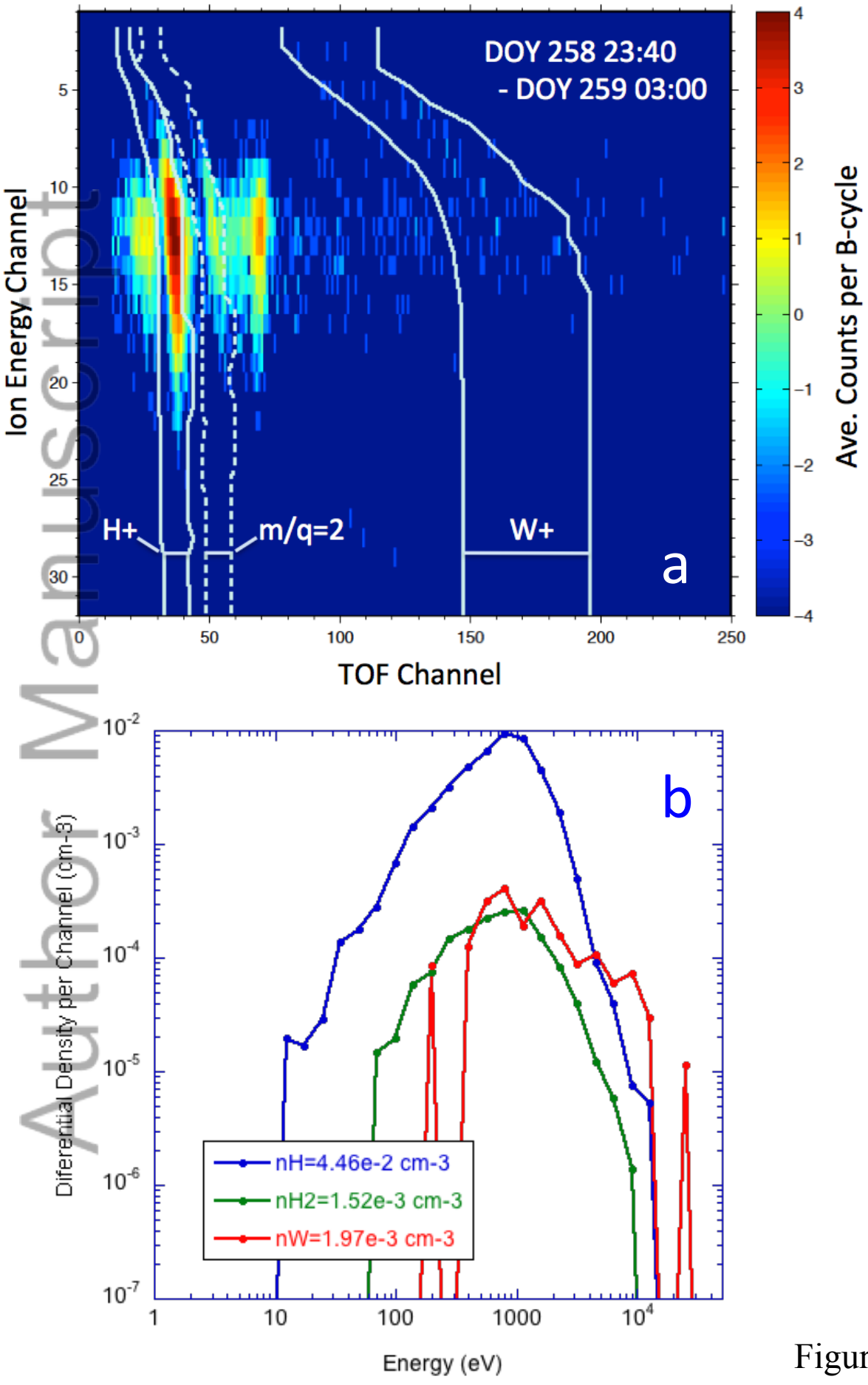

Figure 3

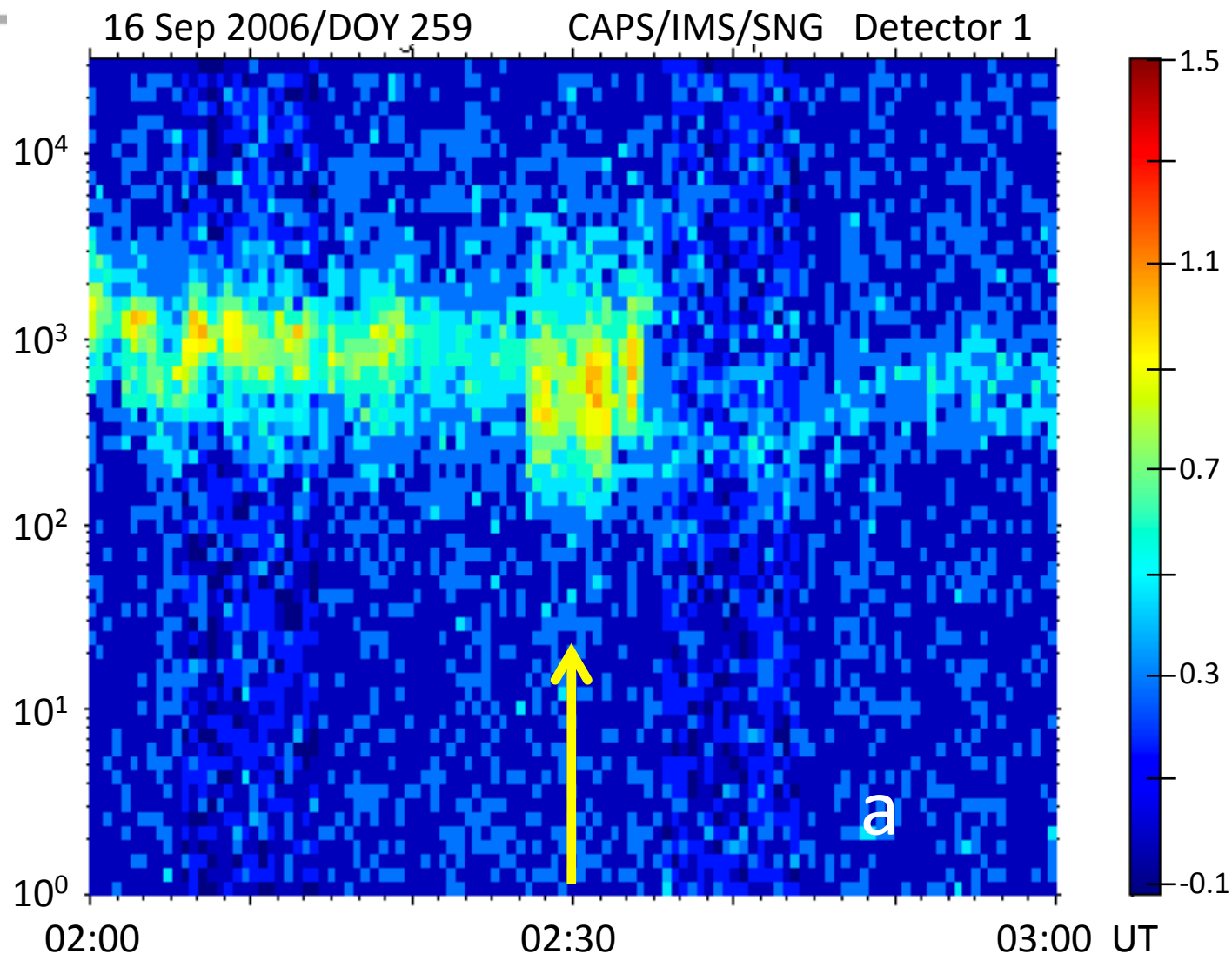

Figure 4a

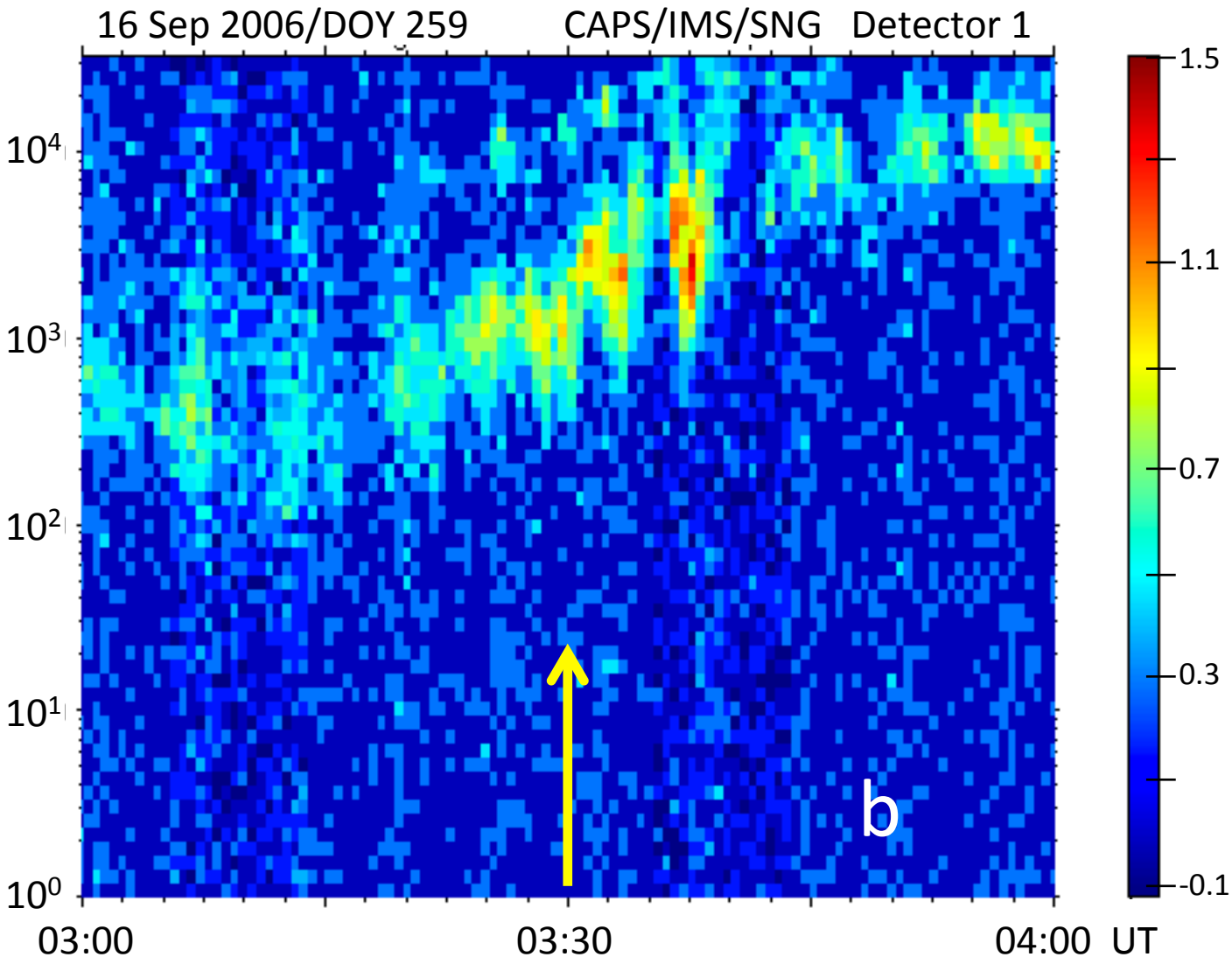

Figure 4b

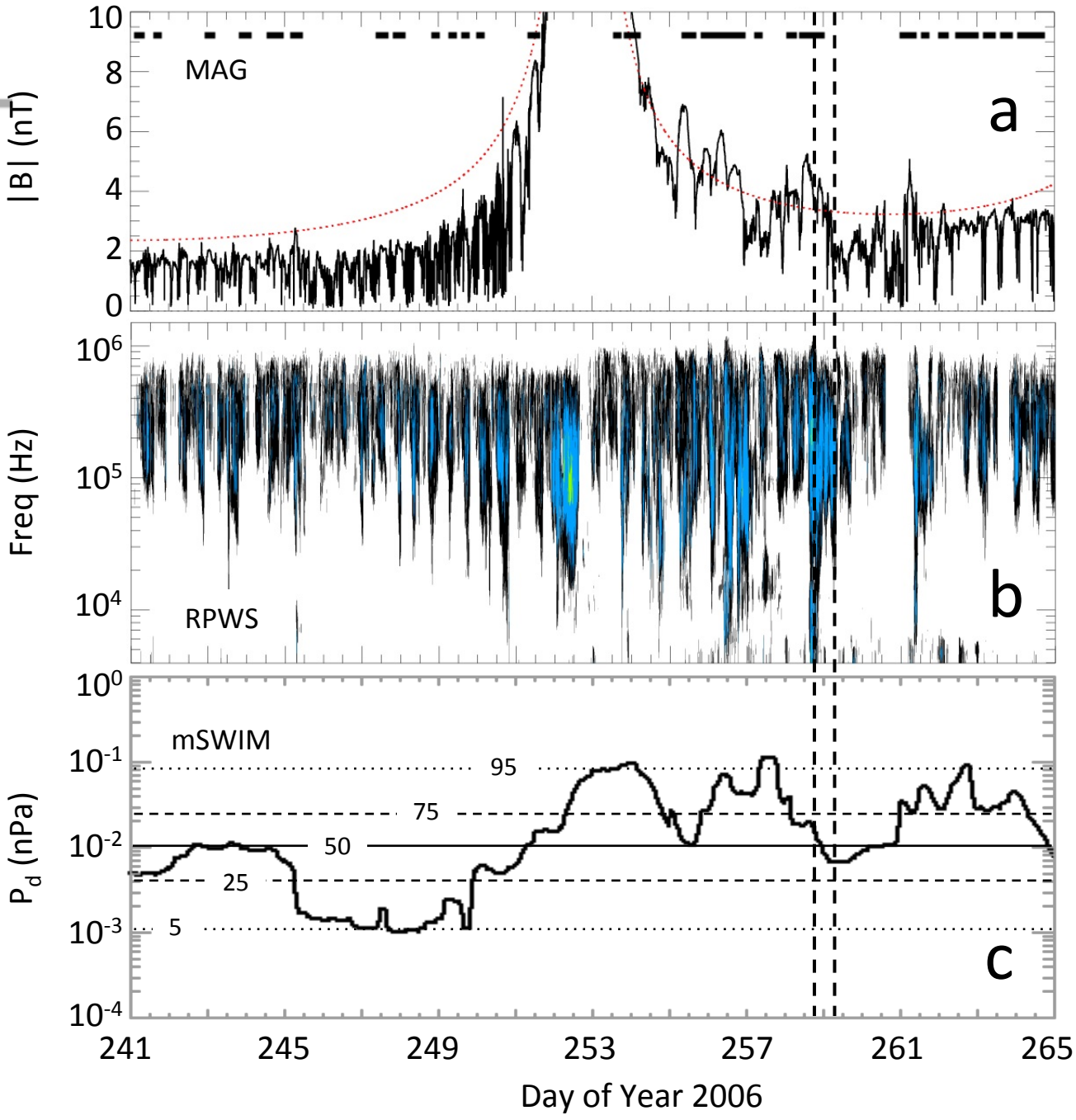

Figure 5

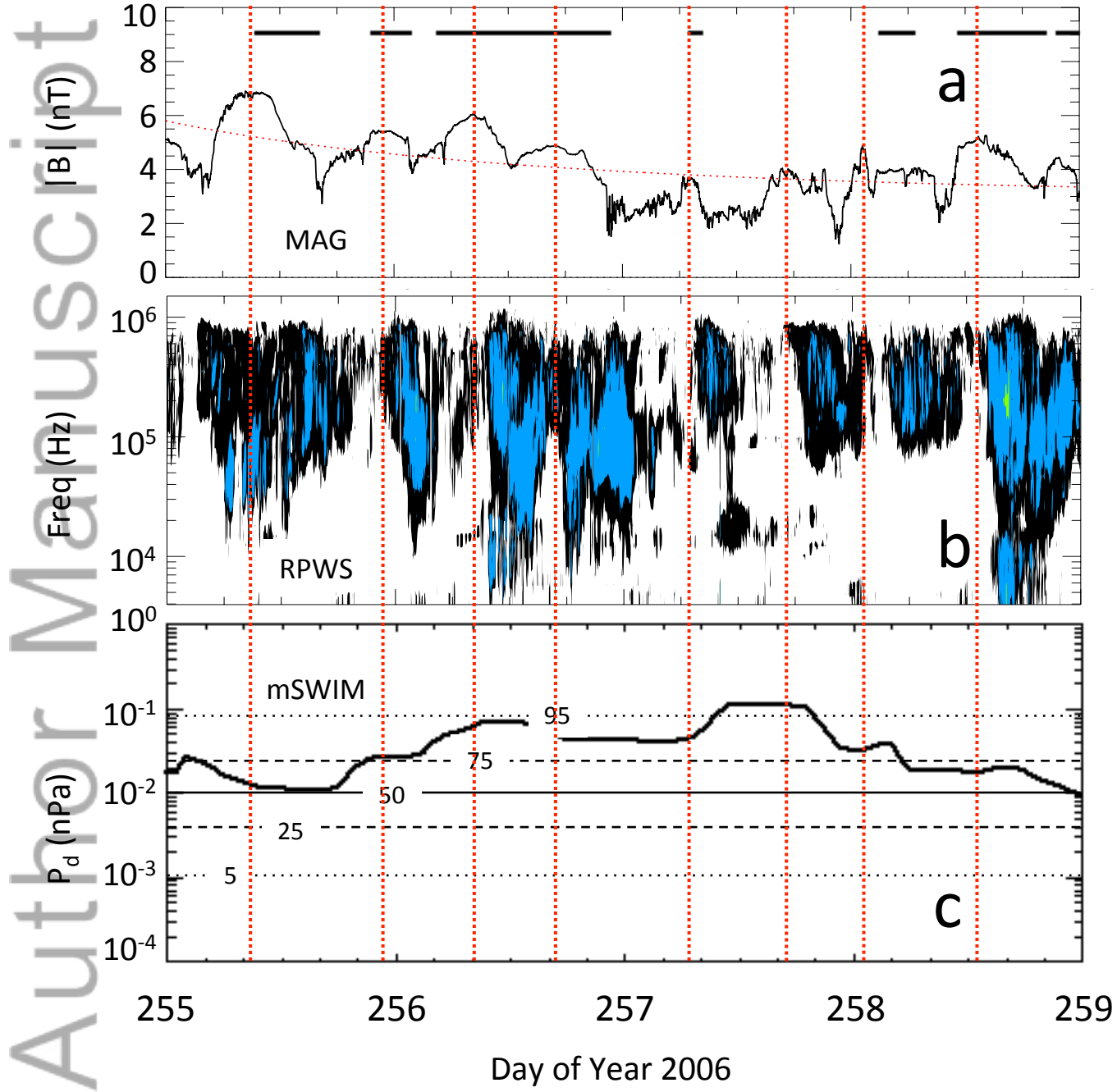

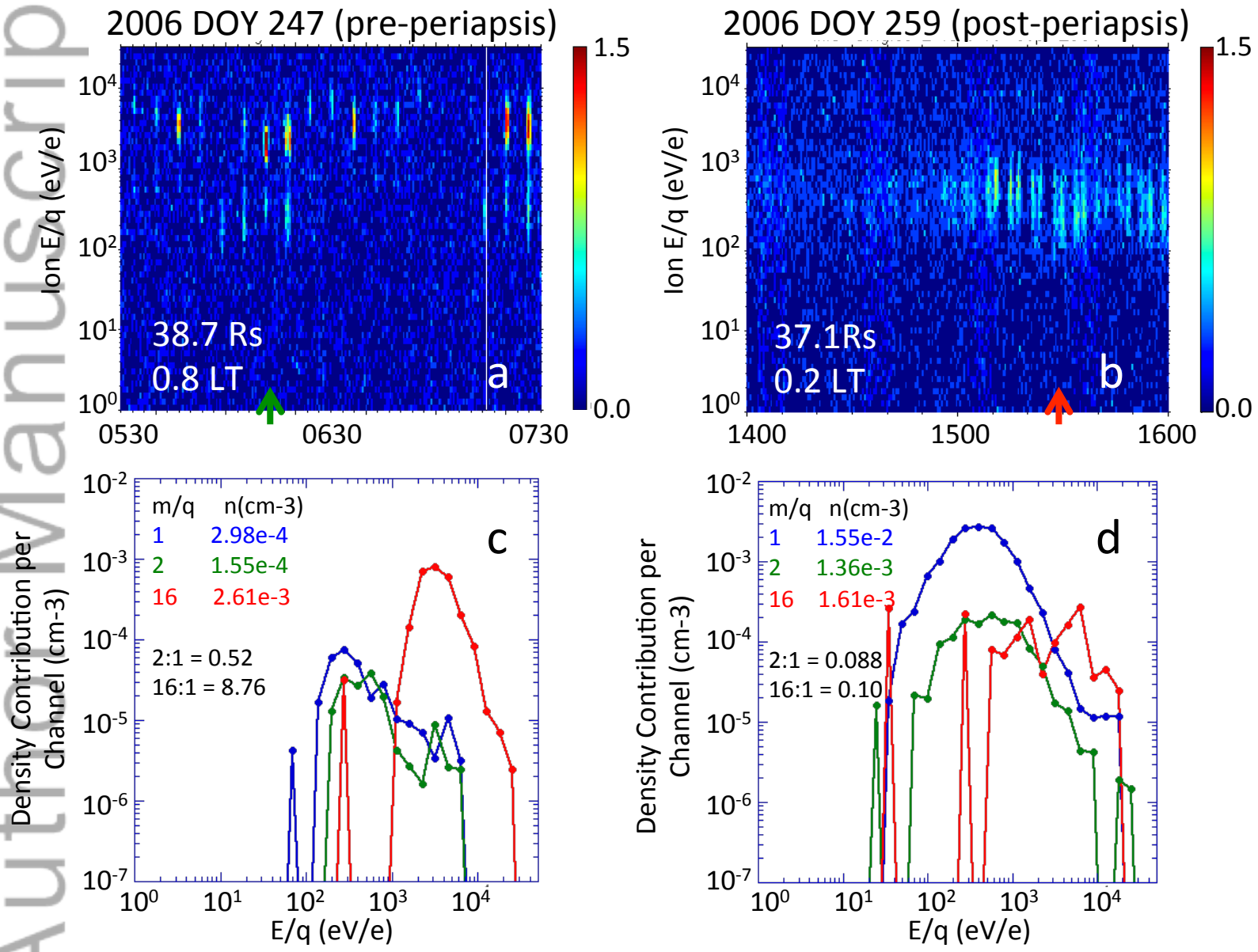

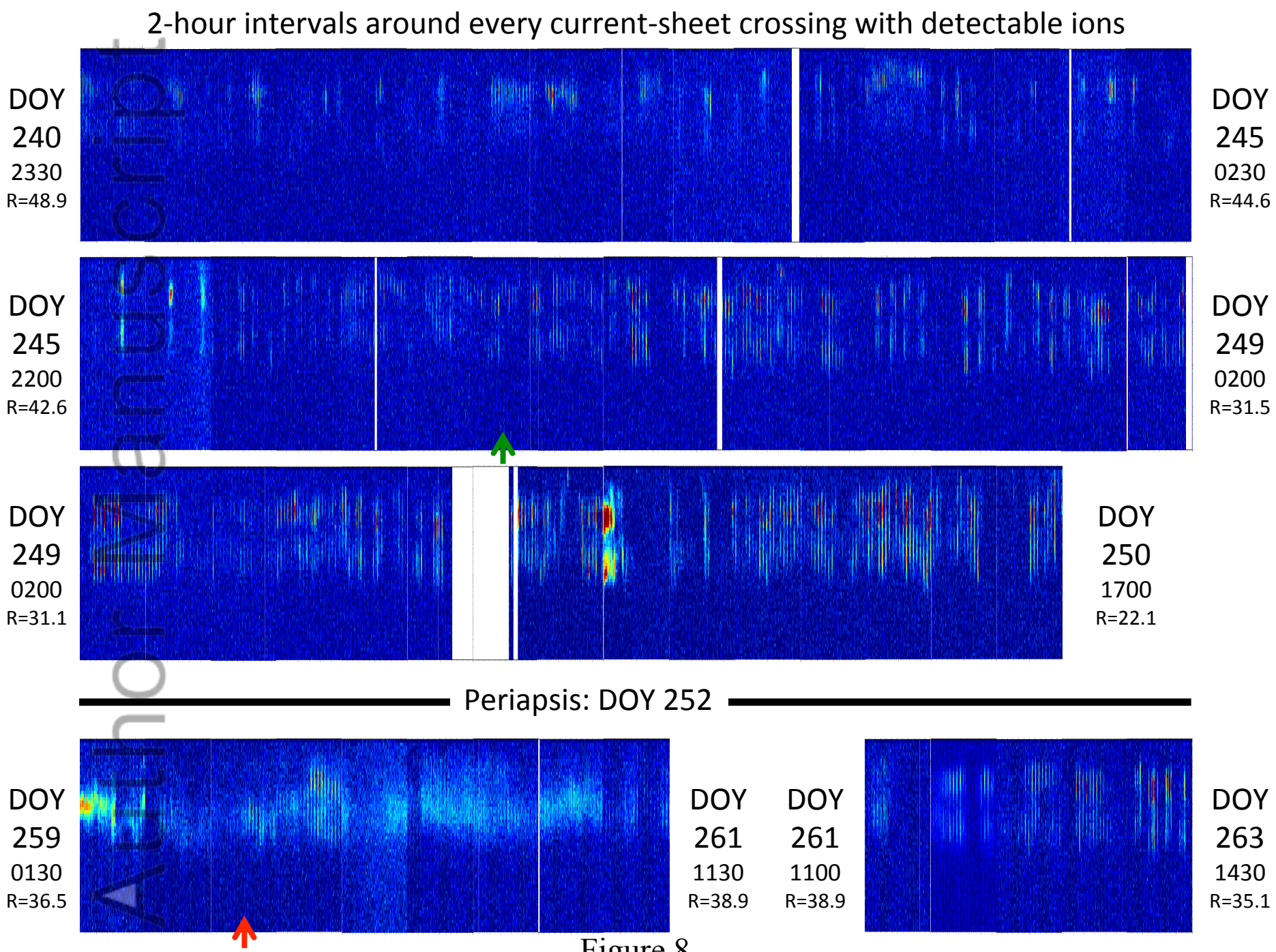

Figure 8